AIChE WILEY InterScience DISCOVER SOMETHING GREAT

PROCESS SYSTEMS ENGINEERING

Approximate Method for Nonlinear Differential and Integrodifferential Equations

Yuriy S. Polyakov
U.S. PolyResearch, Ashland, PA 17921

Viktor V. Dil'man
Kurnakov Institute of General and Inorganic Chemistry, Russian Academy of Sciences, Moscow 119991, Russia

DOI 10.1002/aic.10995
Published online September 8, 2006 in Wiley InterScience (www.interscience.wiley.com).

A generalized variable-parameter averaging (GVPA) method to solve nonlinear differential and integrodifferential equations is formulated. The method uses a constant-parameter solution to the original problem together with averaging and interpolation to obtain approximate solutions to some chemical engineering problems with variable parameters, such as transfer coefficients or permeate velocity. The efficiency of the method is studied with application to the ultrafiltration in dead-end outside-in hollow-fiber modules, filtration in hollow-fiber membrane adsorbers, mass transfer with a variable diffusion coefficient, and concentration polarization in unstirred reverse osmosis batch cells. Comparison with the numerical solutions to the complex chemical engineering problems shows that the solutions obtained by the GVPA method provide a sufficient accuracy in describing the process performance and dramatically cut down the computation time. © 2006 American Institute of Chemical Engineers *AIChE J,* 52: 3813–3824, 2006
Keywords: approximate method, variable-parameter averaging, mathematical modeling, design (process simulation), mass transfer

Introduction

Progress in interdisciplinary studies, deeper understanding of physical mechanisms, development of complex experimental techniques, and outstanding advances in the computer industry caused the focus of theoretical studies in chemical engineering to change from simplified linear to multiparametric nonlinear problems.[1-3] More sophisticated mathematical models require that the dependency of physicochemical parameters and coefficients, such as diffusion, viscosity, and the like, on the process variables be taken into account,[3,4] which significantly complicates the problems under study and often makes it impossible to obtain exact analytical solutions. The idea of a complementary combination of processes has brought about new technologies that are often described by strongly nonlinear mathematical models. Even if the mathematical models for the constituent processes have simple analytical solutions,[1] these nonlinear problems rarely admit exact analytical solutions. As a result, most of the nonlinear problems are usually solved by numerical or approximate methods.[5]

Numerical methods are the most common approach to obtaining accurate solutions to nonlinear problems of chemical engineering.[2,6-8] In many cases, high-speed digital computers allow one to obtain rapid and accurate solutions to many complex scientific and engineering problems. Despite the ubiquity of high-speed computers and availability of many mathematical software packages, however, there are certain limitations in application of numerical methods to nonlinear problems. For example, the theoretical analysis of error, stability, and convergence of numerical approximations to nonlinear problems is usually very complicated, and practically impossible in many cases.[7] As a result, the accuracy of the

Correspondence concerning this article should be addressed to Yu. S. Polyakov at ypolyakov@uspolyresearch.com.

numerical solution is frequently checked by using the other numerical solutions implementing alternative approximation schemes, as well as by the analytical solutions for the particular cases of the problem.[5] Because many chemical engineering problems lead to differential or integrodifferential equations that do not match the templates included in standard mathematical packages, new numerical schemes and special programs implementing the schemes need to be developed. This implies that the knowledge of some advanced topics in computational mathematics and computer science is necessary for successful application of numerical methods to complex engineering problems.[6] It should be noted that because the computational complexity of programs implementing direct numerical methods is usually very high, design and optimization of chemical engineering processes based on numerical solutions may often consume much time.

Approximate methods, which represent the alternative strategy of solving nonlinear engineering problems, are based on the idea of simplifying, or approximating, the original problem to obtain an analytical or fast numerical solution.[4,8] This solution can be used to gain a deeper understanding of the process behavior and accomplish the process design and performance optimization. Sometimes, its accuracy may be comparable with that of numerical solutions.[9,10] The common use of approximate solutions in chemical engineering is explained by the fact that they can be easily implemented as a simple program and can assimilate some error in experimental data caused by instrumental limitations and other reasons. At the same time, the numerical or asymptotic solutions to the problem under study or to its particular cases should be used to obtain a reliable estimate of the accuracy of the approximate methods. Consequently, the numerical and approximate methods in chemical engineering often complement each other in solving nonlinear problems.[9,11]

Generally, six approximate solution approaches, such as weighted residual, integral, asymptotic (perturbation), constant-parameter simplification, model equations, and variable-parameter averaging, are used to solve the nonlinear partial differential and integrodifferential equations arising in chemical engineering.[4,8,12,13]

In the weighted residual, or Galerkin, methods,[4,8] which include such methods as the Bubnov–Galerkin, collocation, and least squares, the approximate solution is written as a linear or nonlinear combination of approximating functions that satisfy the boundary conditions to the original problem. The coefficients of the linear combination are determined by equating the integrals of the product of specially chosen weighted functions by the residual resulting from substituting the approximate expression into the original equation to zero for the whole domain or some subdomain of the problem. Weighted residual methods can often lead to simple analytical expressions. At the same time, their accuracy usually depends on what weighted functions or collocation points are chosen. In this case, the deep understanding of the process and problem is prerequisite for the successful choice of the functions or collocation points.[4] These methods usually fail to provide low-error solutions to nonlinear problems with more than two variable parameters for the whole domain of the problem. However, they can sometimes be used to obtain practically acceptable estimates for some integral characteristics of the problem.[4]

The integral methods,[4,8] which are closely related to the weighted residual methods, typically use one chosen approximating function together with one or several unknown functions to be determined from the appropriate integral relations. Generally, the integral methods are applied to boundary value problems. In many cases, they can provide high accuracy and work for both partial differential and integrodifferential multiparametric equations. For example, they provided sufficiently accurate solutions to nonlinear reverse osmosis and ultrafiltration problems with variable coefficients (diffusion coefficient, membrane selectivity, permeability coefficient).[9,10,14] Given that the main idea of integral methods is to find unknown coefficients (functions) from the integrated equation, they rarely provide simple expressions convenient for theoretical analysis and are helpful only in reducing the computation time, as compared to the more accurate numerical solutions.

The asymptotic approximate methods are based on the asymptotic solutions of the problem to be solved.[4,12,13] They typically include perturbation methods[12,13] and asymptotic techniques.[4,13] These methods can usually give accurate solutions only in some narrow region around the asymptotic limit. The perturbation series often have problems with convergence. As a result, these methods usually fail to adequately describe the solution in the whole domain of the problem. However, they provided some classical approximate analytical solutions in hydrodynamics.[15,16] The methods of asymptotic interpolation and extrapolation, which allow one to build the solution for the whole domain of the problem, are usually ineffective for multiparametric nonlinear problems.[4] At the same time, these problems can use the asymptotic correction technique to improve the accuracy of the other approximate solutions by bringing the latter ones closer to the asymptotic curves.[4]

The constant-parameter simplification (CPS) approach is based on replacing some varying parameter in the problem with its constant value, such as at the initial moment or boundary. In this case, the simplified problem keeps most of the essential features of the original problem. At the same time, this approach can provide low-error solutions only in the close neighborhood of the region for which the constant parameter value was used. Some examples of this technique and its variations are discussed by De et al.[9] and Liu and Williams.[13]

In the model equations approach, the original problem is replaced with a simpler problem based on some physical considerations, estimation of terms in the original equation, some linearization technique, and so forth.[4] For example, a partial differential equation can be replaced with a simplified ordinary differential equation analog. This approach usually requires an in-depth physical understanding of the problem and produces low-error solutions for the profiles of desired functions only for narrow regions rather than for the whole problem domain.[17] At the same time, it can often provide simple analytical expressions for some integral characteristics of the problem.[4] Many problems in hydrodynamics and heat and mass transfer were solved using this approach.[4,15] The classical examples include the deposition of Brownian particles on solid collectors[18-20] and the concentration polarization at phase boundaries in cross-flow reverse osmosis.[21]

The variable-parameter averaging (VPA) methods[4,22] are similar to the CPS methods in that they use the solution to the original problem obtained for the case when one of the variable parameters is taken constant. The constant value is found by

integrating the variable parameter over the whole domain of the problem. These methods can lead to accurate enough estimates for some integral characteristics of the problem, such as the average Sherwood number.[22] At the same time, they rarely provide low-error solutions for local characteristics of the problem such as concentration, heat, and flow velocity profiles.[4]

Various methods of obtaining approximate solutions are often used together to yield a more accurate solution. The examples of these complementary combinations described by Polyanin and Dilman[4] demonstrate that this approach can yield good results for many cases.

The purpose of this study is to present a new method in which the constant-parameter simplification method is combined with variable-parameter averaging to yield low-error expressions for both local and integral characteristics of the problem. It can be applied to several classes of nonlinear partial differential and integrodifferential equations with variable parameters.

Method Formulation

Let us consider a general nonlinear differential or integrodifferential equation:

$$Lu = F[t, \mathbf{x}, u, f(t, \mathbf{x}, u, u_b)] \tag{1}$$

in which L is, as a rule, an arbitrary linear operator; F is an arbitrary function of t, $\mathbf{x}$, u, f; $f(t, \mathbf{x}, u, u_b)$ is, as a rule, a nonlinear function of variable u, which may include derivatives and/or integrals of u, or some function of its boundary values u_b; $\mathbf{x} = \{x_1, \ldots, x_n\}$ is the coordinate vector. The function F can include integrals of $f(t, \mathbf{x}, u, u_b)$ and derivatives of u with respect to the coordinates $\{x_1, \ldots, x_n\}$ and/or time t. Integral operators can appear only on the right side of Eq. 1. $f(t, \mathbf{x}, u, u_b)$ may also appear in one of the boundary conditions.

This type of equation with appropriate initial and boundary conditions is widely encountered in problems of physicochemical hydrodynamics and chemical engineering, and its solution is strongly complicated given the nonlinear dependency of F on u.[4] Therefore, the idea of developing an approximate method of solving the general Eq. 1, using the analytical or low-error approximate solutions to its linear (constant parameter) case together with iterative algorithms and interpolation techniques, is of current interest.

Let us replace $f(t, \mathbf{x}, u, u_b)$ with a constant value $\langle f \rangle$, which is obtained by averaging $f(t, \mathbf{x}, u, u_b)$ over some domain of t and $\mathbf{x}$, and then find a solution to the simplified problem

$$Lu = F(t, \mathbf{x}, u, \langle f \rangle) \tag{2}$$

assuming that Eq. 2 with the initial and boundary conditions related to Eq. 1 has an exact analytical, or low-error approximate (numerical), solution. If one of the boundary conditions depends on $f(t, \mathbf{x}, u, u_b)$, the latter is also replaced with $\langle f \rangle$.

The value of $\langle f \rangle$ at time t and the boundary of S can be determined by solving the integral equation

$$\langle f \rangle = \frac{1}{tS} \int_0^t \int_S f(t_1, \mathbf{x}, u[t_1, \mathbf{x}, \langle f \rangle]) \delta S dt_1 \tag{3}$$

using the iterative algorithm

$$\langle f \rangle^{(i+1)} = \frac{1}{tS} \int_0^t \int_S f(t_1, \mathbf{x}, u[t_1, \mathbf{x}, \langle f \rangle^{(i)}]) \delta S dt_1 \tag{4}$$

which virtually represents the method of successive approximations.[23] Here, S is the length, or surface area, or volume, depending on the dimension of the problem under study. Equations 3 and 4 use the dependency of u obtained by solving Eq. 2 with appropriate boundary and initial conditions. The initial, or boundary, value or the value obtained for the preceding time (or coordinate) interval can be used as $\langle f \rangle^0$ to accelerate the convergence of algorithm 4.

The main idea of the method is based on the observation that for several nonlinear chemical engineering problems, the approximate curve of f calculated using u determined from Eq. 2 approaches the accurate numerical solution for f at the end of the averaging interval, and Eq. 3 basically represents the mathematical formulation of this fact.

For example, when the time dependency of function u is to be found, Eq. 3 is solved for the time point t; that is, for the end point of the interval $[0, t]$ for which the value of $\langle f \rangle$ was determined. When the relation between $\langle f \rangle$ and t cannot be obtained as an explicit analytical solution to Eq. 3, it can be found by determining the values of $\langle f \rangle$ for several (3 or 4) values of t from Eq. 3 with the help of an iterative algorithm (Eq. 4) and then by using the method of asymptotic interpolation[24] to build the whole curve and find the constant coefficients in the interpolation formula.

Given that many one-dimensional unsteady problems of chemical engineering described by Eq. 2 have exact analytical solutions, they are best suited for illustrating and testing the approximate method that will be called the *generalized variable-parameter averaging* (GVPA) method. In this case, Eqs. 1–3 are rewritten as

$$Lu = F[t, x_1, u, f(t, x_1, u, u_b)] \tag{5}$$

$$Lu = F(t, x_1, u, \langle f \rangle) \tag{6}$$

$$\langle f \rangle = \frac{1}{t(x_1 - a)} \int_0^t \int_a^{x_1} f(t_1, x, u[t_1, x, \langle f \rangle]) dx dt_1 \tag{7}$$

where x_1 is the coordinate and a is its lower boundary.

If the boundary dependency of u on t is to be found, then Eq. 7 transforms to

$$\langle f \rangle = \frac{1}{t} \int_0^t f(t_1, p, u[t_1, p, \langle f \rangle]) dt_1 \tag{8}$$

where $p = \{a, q\}$ and where q is the upper boundary of x_1.

On the other hand, if the profile of u is to be found for a particular value of $t = T$, then Eq. 7 can be written as

$$\langle f \rangle = \frac{1}{x_1 - a} \int_a^{x_1} f(T, x, u[T, x, \langle f \rangle])dx \tag{9}$$

Integral characteristics can be determined either from function f or by using function u with $\langle f \rangle$ substituted before or after the integration. The particular choice depends on the accuracy of the solution and/or the availability of simple analytical expressions.

All other unknown functions can be calculated either from $f(t, x_1, u[t, x_1, \langle f \rangle])$ or $u[t, x_1, \langle f \rangle]$.

Let us consider the application of the GVPA approximate method to some one-dimensional unsteady problems of mass transfer described by Eq. 5 that have exact analytical solutions to Eq. 6.

Ultrafiltration in Dead-end Outside-in Hollow-Fiber Filter

A flow diagram for the ultrafiltration in a dead-end outside-in hollow-fiber filter is shown in Figure 1.[25,26] The suspension to be clarified moves from the periphery of the filter to its axis. The suspension is filtered by forcing the liquid through the porous hollow-fiber membranes under the action of transmembrane pressure gradient. The clarified water produced in the hollow-fiber lumens is called the permeate. The retained particles deposit on the hollow-fiber shells.[25,26] As the suspension flows to the filter axis, the concentration of suspended particles decreases as a result of the formation of deposit on the hollow-fiber shells. On the other hand, the concentration increases as a result of the withdrawal of permeate from the hollow-fiber lumens.

The growth of the cake layer on the membrane surface can be described by an equation that is mathematically equivalent to the linear equation of reversible adsorption. In this case, the phenomenological constants determined with the help of experimental curves of permeate flow rate vs. time play the role of the adsorption and desorption coefficients.

The system of equations describing the filtration of suspensions in the filter can be written as[25,26]

$$\frac{\partial c}{\partial t} - \frac{1}{r}\frac{\partial (rwc)}{\partial r} = -s\frac{\partial \Gamma}{\partial t} \tag{10}$$

$$\frac{\partial \Gamma}{\partial t} = \beta c - \alpha \Gamma \tag{11}$$

$$w = \frac{1}{r}\int_{r_{in}}^{r} sV_p r dr \tag{12}$$

$$V_p = \frac{\Delta P}{\mu(R_m + r_c \Gamma)} \tag{13}$$

where c is the concentration of suspended particles; t is the time; w is the liquid velocity in the channels between hollow fibers; r is the radial coordinate; s is the ratio of hollow-fiber membrane shell area to the suspension volume inside the filter; Γ is the specific cake deposit (cake mass per square meter of hollow-fiber membrane shell area); β, α are the coefficients of adsorption and peptization, respectively; V_p is the permeate velocity; ΔP is the transmembrane pressure; μ is the liquid viscosity; $R_m = \Delta P/(\mu V_0)$, the clean membrane resistance; r_c is the specific cake resistance; and V_0 is the initial permeate velocity.

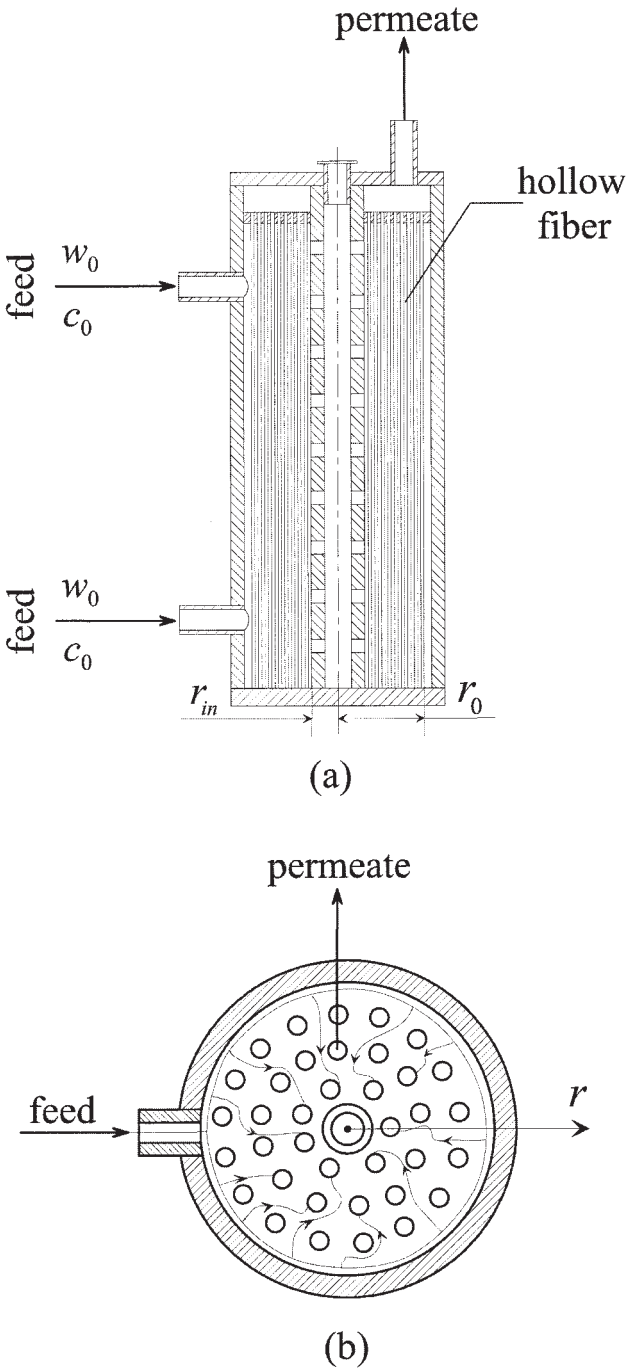

Figure 1. Dead-end outside-in hollow-fiber membrane filter.[26]

(a) Flow diagram in vertical cross section; (b) flow diagram in horizontal cross section.

Equations 10–13 allow us to describe the unsteady profile of the suspension concentration c running across the filter and the

growth of specific cake deposit Γ on the filtering outside surfaces of hollow fibers. To simplify the calculations and generalize their results to a rectangular dead-end outside-in hollow-fiber filter, an effective axial (filter depth) coordinate z and effective depth d are introduced[26]:

$$z = (r_0^2 - r^2)/(2r_0) \qquad d = (r_0^2 - r_{in}^2)/(2r_0) \tag{14}$$

This transforms Eqs. 10 and 12 to

$$\frac{\partial c}{\partial t} + \frac{\partial (cw)}{\partial z} = -s\frac{\partial \Gamma}{\partial t} \tag{15}$$

$$w = \int_z^d sV_p dz \tag{16}$$

The problem will be solved on the assumption that the concentration at the filter inlet remains constant. The initial and boundary conditions are taken as

$$z = 0,\ t > 0 \qquad c = c_0 \qquad z > 0,\ t = 0 \qquad c = \Gamma = 0 \tag{17}$$

The permeate productivity of the filter is defined as

$$\frac{V}{V_0} = \frac{1}{d}\int_0^d \frac{dz}{1 + \chi_1 \Gamma} \tag{18}$$

where $\chi_1 = r_c/R_m$.

The problem in dimensionless form can be written as

$$\frac{\partial^2 \gamma}{\partial \tau^2} + (1 + N_\alpha)\frac{\partial \gamma}{\partial \tau} = -\frac{1}{N_\beta}\frac{\partial}{\partial Z}\left[\left(\frac{\partial \gamma}{\partial \tau} + N_\alpha \gamma\right) \times \int_Z^1 \nu(\gamma) dZ\right] \tag{19}$$

$$Z = 0,\ \tau > 0 \qquad \gamma = [1 - \exp(-N_\alpha \tau)]/N_\alpha$$
$$Z > 0,\ \tau = 0 \qquad \gamma = \partial \gamma/\partial \tau = 0 \tag{20}$$

where $\gamma = \Gamma(s/c_0)$, $N_\beta = \beta/V_0$, $\tau = s\beta t$, $Z = z/d$, $N_\chi = \chi_1 c_0/s$, $N_\alpha = \alpha/(s\beta)$, and $v = V_p/V_0$.

The dimensionless permeate velocity takes the form

$$\nu = \frac{1}{1 + N_\chi \gamma} \tag{21}$$

Application of the GVPA method to the function v in Eq. 19 gives

$$\frac{\partial^2 \gamma}{\partial \tau^2} + (1 + N_\alpha)\frac{\partial \gamma}{\partial \tau} = -\frac{1}{N_\beta}\frac{\partial}{\partial Z}\left[\left(\frac{\partial \gamma}{\partial \tau} + N_\alpha \gamma\right) \times \langle \nu \rangle (1 - Z)\right] \tag{22}$$

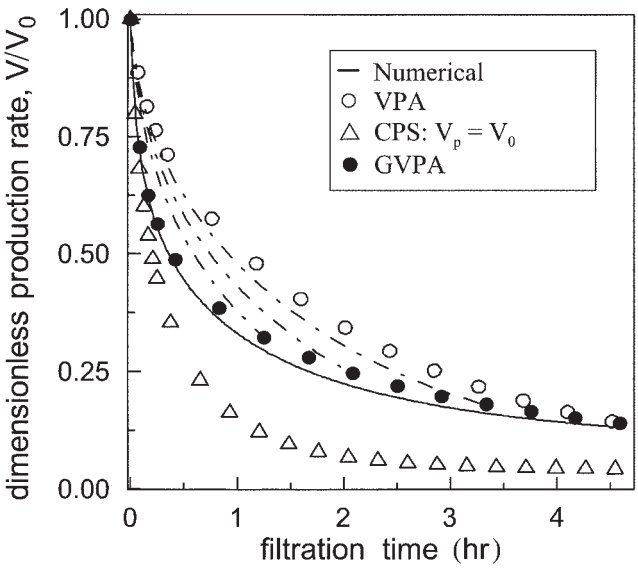

Figure 2. Decline of dead-end filter permeate flow rate with time.

$N_\beta = 2.6$, $N_\chi = 0.0072$, $s\beta = 0.7\ s^{-1}$, $N_\alpha = 0.0006$.

$$\langle \nu \rangle = \frac{1}{\tau}\int_0^\tau \int_0^1 \frac{1}{1 + N_\chi \gamma(Z,\ \tau_1,\ \langle \nu \rangle)}\, dZ d\tau_1 \tag{23}$$

Here, the upper limit in the integral with respect to Z is equal to unity because the performance parameter of the filter, permeate productivity, is to be determined. Problem given by Eqs. 20 and 22 can be solved using the Laplace transform[26]:

$$\gamma = 0 \qquad \text{when } \tau < N_\beta^* X \tag{24}$$

$$\gamma = (N_\alpha)^{-1}\exp[X - N_\alpha \tau - N_\beta^* X + N_\alpha N_\beta^* X] \times \sum_{m=1}^{\infty} I_m[2\sqrt{N_\alpha N_\beta^* X(\tau - N_\beta^* X)}]\left[\frac{N_\alpha(\tau - N_\beta^* X)}{N_\beta^* X}\right]^{m/2}$$
$$\text{when } \tau > N_\beta^* X \tag{25}$$

where $N_\beta^* = N_\beta/\langle \nu \rangle$ and $X = -\ln(1 - Z)$.

The calculated values of $\langle \nu \rangle$ were interpolated as a function of time using the method proposed by Vyaz'min et al.[24] In this case, the three-point interpolation formula was selected:

$$\langle \nu \rangle = (1 + a_1 \tau^{a_2})^{-a_3} \tag{26}$$

where a_1, a_2, and a_3 are positive constant coefficients.

Figure 2 demonstrates the comparison between the numerical solution[25,26] and the analytical solution for the case of a constant membrane velocity equal to its initial value; the approximate solution, in which $\langle \nu \rangle$ is determined using the whole time interval (this method virtually belongs to the family of VPA methods); and the GVPA method.

It is seen that direct use of the analytical solution (Eqs. 24 and 25) for Γ obtained for the case of constant $V_p = V_0$ in determining the time dependency of the filter productivity

yields a significant error, underestimating the productivity. The VPA method, in which the curve of Γ is determined using the time- and coordinate-averaged value of permeate velocity calculated for the whole process time interval, gives a noticeable error in determining the productivity, generally overestimating its value. It should be noted that this error diminishes at the end of the computation interval. In the GVPA method, the desired permeate productivity is built using the end points of the curves calculated for smaller intervals (for illustration, see the dot–dash lines in Figure 2). It is obvious that the GVPA method gives a curve close enough to the numerical solution: its maximum error does not exceed 13%.

The relatively low error in determining the productivity by the GVPA method as compared to the numerical solution is attributed to the behavior of the permeate velocity. At the initial moment of time, the instantaneous values of permeate velocity, and thus productivity, in the numerical method are higher than its averaged value taken for the approximate solution. As a result, the decline in the actual permeate productivity is higher than that for the approximate curve.[27] In the region of intermediate times, the instantaneous values of permeate velocity in the numerical method become closer to the averaged value in the approximate method. Consequently, the declines in permeate productivity for both methods become comparable. At the end region, the instantaneous values in the numerical method are lower than the averaged value in the approximate method. Consequently, the decline in permeate productivity for the approximate method is higher than that for the numerical method. As a result, the error arising at the first half of the curve is partially compensated by the opposite-sign error produced at the second half. Therefore, the error for the end point of the approximate curve can be the least.

Filtration in Hollow-Fiber Membrane Adsorber

The next example illustrating the application of the GVPA method is a cross-flow ultrafiltration hollow-fiber filter (Figure 3) that produces two clarified streams: permeate and filtrate, the latter of which is produced as a result of the deposition of particles on the membrane surface, much like it takes place in depth filtration and adsorption.[28-30] The filtrate flow rate in this filter, which is called the hollow-fiber membrane (HFM) adsorber, is adjusted by the control valve mounted at the adsorber filtrate outlet.

The HFM adsorber differs from a conventional depth filtration or adsorption filter in that the value of liquid flow rate does not remain constant across the HFM adsorber. It declines as the suspension runs deeper to its axis because of the withdrawal of permeate through the semipermeable walls of hollow fibers. The decline in permeate flow rate caused by the hydraulic resistance of the cake layer of deposited particles growing on the membrane surfaces is compensated by the equal increase in filtrate flow rate. This provides a constant productivity equal to the initial permeate flow rate at constant transmembrane pressure. The filtration cycle is interrupted for membrane flushing when the concentration of suspended particles in the mixture of permeate and filtrate reaches a given upper limit.

Mathematically, the problem formulation for the HFM adsorber differs from that for the dead-end outside-in hollow-fiber filter only in the form of continuity Eq. 16. For the adsorber, it is written as

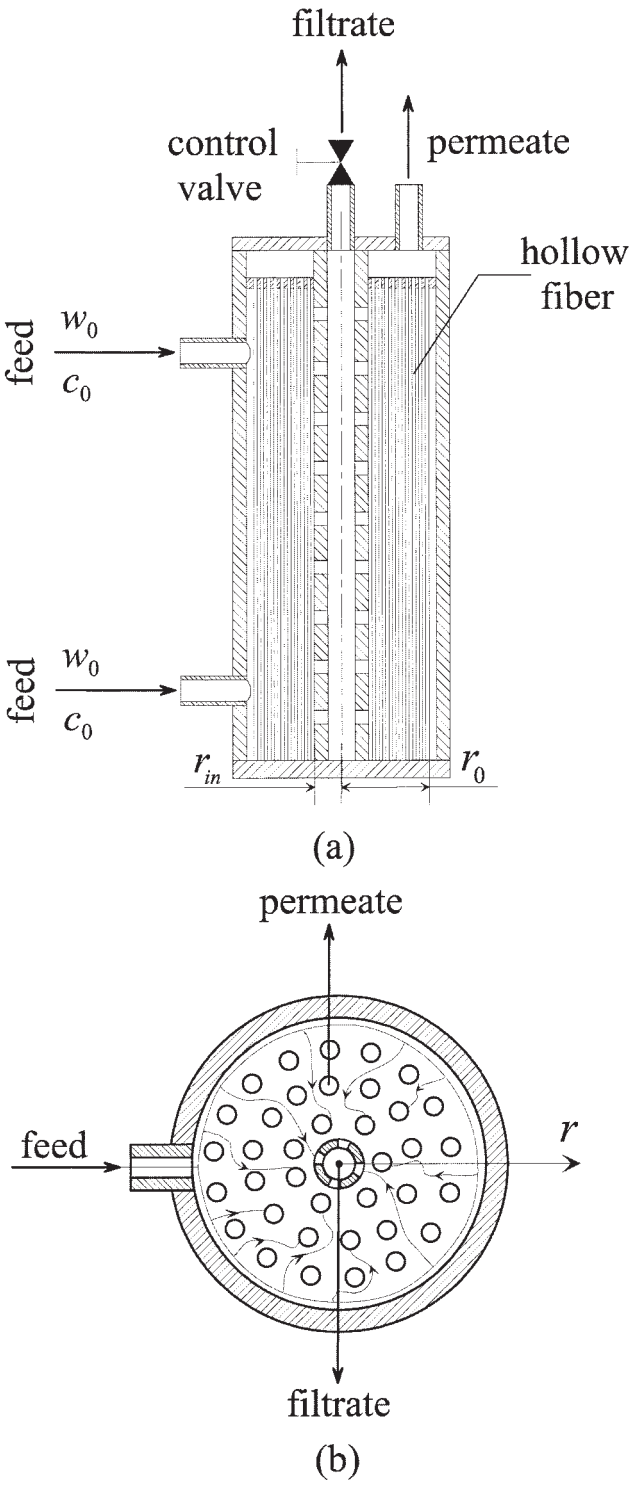

Figure 3. Hollow-fiber membrane adsorber.

(a) Flow diagram in vertical cross section; (b) flow diagram in horizontal cross section.

$$w = w_0 - \int_0^z sV_p dz \tag{27}$$

The main performance characteristics of an HFM adsorber are the permeate velocity averaged over the adsorber depth

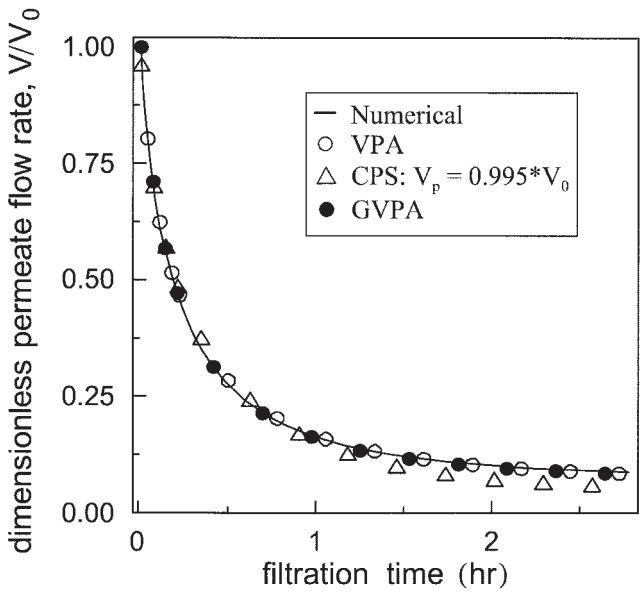

Figure 4. Decline of adsorber permeate flow rate with time.

$\beta = 1.81 \times 10^{-4}$ m/s, $\alpha = 4.2 \times 10^{-4}$ s^{-1}, $s = 3.88 \times 10^{3}$ m^{-1}, $V_0 = 6.94 \times 10^{-5}$ m/s, $\xi = 1$, $d = 0.05$ m, $N_\chi = 0.0072$.

$$\frac{V}{V_0} = \frac{1}{d}\int_0^d \frac{dz}{1 + \chi_1 \Gamma} \tag{28}$$

and the concentration of suspended particles at the adsorber outlet

$$c_f = \frac{1}{\beta}\left[\frac{\partial \Gamma(t, d)}{\partial t} + \alpha \Gamma(t, d)\right] \tag{29}$$

The differential equation in dimensionless form for this process is written as

$$\frac{\partial^2 \gamma}{\partial \tau^2} + (1 + N_\alpha)\frac{\partial \gamma}{\partial \tau} + \frac{1}{N_\beta} \times \frac{\partial}{\partial Z}\left\{\left(\frac{\partial \gamma}{\partial \tau} + N_\alpha \gamma\right) \times \left[1 - \xi \int_0^Z \nu(\gamma) dZ\right]\right\} = 0 \tag{30}$$

Equation 30 will be solved for the following initial and boundary conditions:

$$\begin{aligned} Z = 0 \qquad \tau > 0 \qquad \gamma &= [1 - \exp(-N_\alpha \tau)]/N_\alpha \\ Z > 0 \qquad \tau = 0 \qquad \gamma &= \partial \gamma / \partial \tau - 0 \end{aligned} \tag{31}$$

Here, $\xi = sV_0 d/w_0$ and $N_\beta = s\beta d/w_0$. The other dimensionless parameters are the same as in the first example.

Application of the GVPA method to the function v in Eq. 30 gives

$$\frac{\partial^2 \gamma}{\partial \tau^2} + (1 + N_\alpha)\frac{\partial \gamma}{\partial \tau} = -\frac{1}{N_\beta}\frac{\partial}{\partial Z}\left[\left(\frac{\partial \gamma}{\partial \tau} + N_\alpha \gamma\right) \times (1 - \xi \langle \nu \rangle Z)\right] \tag{32}$$

$$\langle \nu \rangle = \frac{1}{\tau Z}\int_0^\tau \int_0^Z \frac{1}{1 + N_\chi \gamma(Z_1, \tau_1, \langle \nu \rangle)} dZ_1 d\tau_1 \tag{33}$$

The solution to the problem (Eqs. 31 and 32), which can be obtained using the Laplace transform,[28] is written as

$$\gamma = 0 \qquad \text{when } \tau < N_\beta X \tag{34}$$

$$\gamma = (N_\alpha)^{-1} \exp[\xi_{av} X - N_\alpha \tau - N_\beta X + N_\alpha N_\beta X] \times \sum_{m=1}^{\infty} I_m[2\sqrt{N_\alpha N_\beta X(\tau - N_\beta X)}]\left[\frac{N_\alpha(\tau - N_\beta X)}{N_\beta X}\right]^{m/2}$$

$$\text{when } \tau > N_\beta X \tag{35}$$

where $\xi_{av} = \xi \langle v \rangle$ and $X = -\ln(1 - \xi_{av} Z)/\xi_{av}$.

As in the first example, the function $\langle v \rangle$ can be interpolated with the help of Eq. 26.

In addition to the direct computation of the adsorber performance characteristics using the calculated profile of Γ (filled and unfilled circles in Figures 4 and 5), the filtrate concentration will also be determined using the formula resulting from the integral equations for the mass conservation law (unfilled squares in Figure 5)[28]:

$$c_f = \left(c_0 w_0 - s\int_0^d \frac{\partial \Gamma}{\partial t} dz - \int_0^d \frac{\partial c}{\partial t} dz\right) \Big/ \left(w_0 - \int_0^d s V_p dz\right) \tag{36}$$

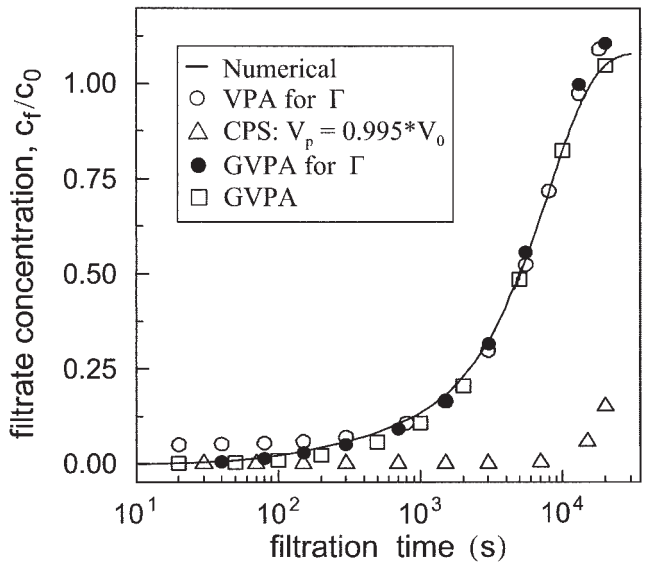

Figure 5. Dependency of filtrate concentration on time.

$\beta = 1.81 \times 10^{-4}$ m/s, $\alpha = 4.2 \times 10^{-4}$ s^{-1}, $s = 3.88 \times 10^{3}$ m^{-1}, $V_0 = 6.94 \times 10^{-5}$ m/s, $\xi = 1$, $d = 0.05$ m, $N_\chi = 0.0072$.

It is seen from Figure 4 that both the VPA and GVPA methods can describe the adsorber permeate flow rate with a sufficient accuracy. Their maximum error relative to the numerical solution is at most 4–5%.[30] At the same time, the CPS equation for determining Γ with a constant permeate velocity $V_p = 0.995V_0$ noticeably underestimates the permeate flow rate at intermediate and high values of time.

Because it follows from the calculated curves for the filtrate concentration shown in Figure 5, which is the most important performance characteristic determining the duration of filtration cycles and thus the moments of their interruptions for membrane flushing, the GVPA method is the only approximate procedure that gives a low error. The VPA method highly overestimates the filtrate concentration at low values of time, coming closer to the numerical solution as the time approaches intermediate values. The CPS method for determining Γ with $V_p = 0.995V_0$ underestimates c_f almost from the beginning of the process, deviating from the numerical solution more and more as the time increases. It should be noted that the GVPA method using the calculated profile for Γ gives a lower error at the beginning of the process as compared to the GVPA method using Eq. 36. At the same time, the GVPA method for Γ starts to significantly deviate from the numerical curve at the time of breakthrough.

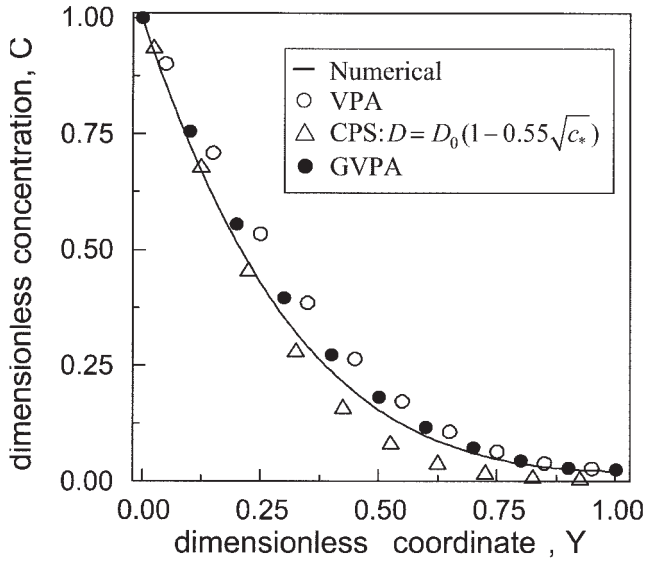

Figure 6. Concentration profile along the coordinate.

$\tau = 0.1$.

Mass Transfer with Variable Diffusion Coefficient

The third example is the problem with variable molecular diffusion coefficient D, which is a function of the solution concentration c.[4] In chemical engineering processes, the dependency of D on c can considerably affect the rate of mass transfer. The study of this effect is complicated by the fact that there is no universal relation to describe the dependency of D on c for liquids.[4,31]

For dilute salt solutions, the experimental data on the dependency of D on c can be satisfactorily described by the relation[22,31]

$$D = D_0(1 - b\sqrt{c}) \tag{37}$$

where D_0 is the diffusion coefficient in an infinitely diluted solution and b is a constant coefficient.

The equation describing the unsteady one-dimensional mass transfer by diffusion in a process where D is governed by Eq. 37 can be written as

$$\frac{\partial c}{\partial t} = \frac{\partial}{\partial y}\left[D_0(1 - b\sqrt{c})\frac{\partial c}{\partial y}\right] \tag{38}$$

Its solution will be sought for the following initial and boundary conditions:

$$\begin{array}{lllll} t = 0 & 0 \le y \le H & c = 0 & & \\ t > 0 & y = 0 & c = c_* & y = H & \partial c/\partial y = 0 \end{array} \tag{39}$$

The numerical solution to the problem of Eqs. 38 and 39, which will be used to estimate the accuracy of the approximate method, can be obtained using the *pdepe* function built into the standard mathematical package Matlab (The MathWorks, Natick, MA).

The problem of Eqs. 38–39 in dimensionless form with the diffusion coefficient D averaged over time and coordinate is written as

$$\frac{\partial C}{\partial \tau} = \langle D \rangle \frac{\partial^2 C}{\partial Y^2} \tag{40}$$

$$\langle D \rangle = \frac{1}{\tau Y}\int_0^{\tau}\int_0^{Y}(1 - B\sqrt{C[Y_1, \tau_1, \langle D \rangle]})dY_1 d\tau_1 \tag{41}$$

$$\begin{array}{lllll} \tau = 0 & 0 \le Y \le 1 & C = 0 & & \\ \tau > 0 & Y = 0 & C = 1 & Y = 1 & \partial C/\partial Y = 0 \end{array} \tag{42}$$

where $C = c/c_*$ $Y = y/H$, $\tau = D_0 t/H^2$, and $B = b\sqrt{c_*}$

The problem in Eqs. 40 and 42 has an exact analytical solution[4]:

$$C = 1 + \frac{4}{\pi}\sum_{m=0}^{\infty}\frac{(-1)^{m+1}}{2m+1}\exp\left[-\frac{\pi^2}{4}(2m+1)^2\langle D \rangle \tau\right]\cos\left[\frac{\pi}{2}(2m + 1)(1 - Y)\right] \tag{43}$$

To compare the numerical and approximate solutions, we will use the experimental relation $D = D_0(1 - 0.55\sqrt{c})$ recommended for some monovalent salt solutions with a molar concentration $c \le 0.1$ M.[4]

Figures 6 and 7 illustrate the variation of the dimensionless concentration with dimensionless coordinate and time. The

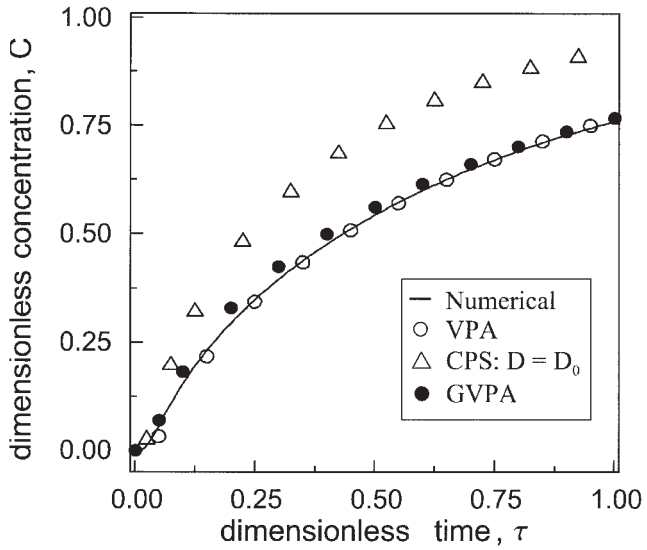

Figure 7. Dependency of concentration on time.

$Y = 0.5$.

dependency of $\langle D \rangle$ on coordinate Y is described by the interpolation equation

$$\langle D \rangle = (1 - B)\exp[-a_1 Y^p] + (1 - \exp[-a_2 Y^q])$$

The dependency of $\langle D \rangle$ on time τ is described by the interpolation equation

$$\langle D \rangle = [1 + a_1(1 - \exp[-a_2 \tau^r])]^{-1}$$

Here, a_1, a_2, p, q, and r are positive constant coefficients.

It is obvious that the GVPA method describes well the concentration profile along the coordinate over its whole range (Figure 6). At the same time, the VPA method yields a noticeable error, overestimating the values of concentration for the intermediate values of coordinate. Note that the CPS method, Eq. 43 with $D = D_0(1 - 0.55\sqrt{c_*})$, can satisfactorily describe the concentration profile only within a small region near the interface ($Y = 0$), considerably underestimating the values of concentration as the distance from the interface increases.

The profile of concentration vs. time is described well by both the GVPA and VPA methods (Figure 7). Equation 43 with $D = D_0$ significantly overestimates the value of concentration from the very beginning of the process.

Concentration Polarization in Unstirred Reverse Osmosis Batch Cell

The last example is the problem of concentration polarization in a reverse osmosis batch cell without axial flux equipped with a flat membrane (Figure 8). This cell is a convenient model for studying isothermal diffusion mass transfer from the membrane surface. A salt solution with concentration c_0 is supplied to the cell by inlet 6 under pressure ΔP and runs normally to membrane surface 3, where it is separated into a permeate (almost pure water that passed through the membrane pores) and salt molecules retained at the membrane surface. The concentration gradient arising at the membrane surface brings about a diffusion flux that transports the salt molecules retained at the membrane surface back to the solution core, forming an unsteady one-dimensional profile of the salt concentration. The concentration at an infinite distance from the membrane surface is assumed to be constant and equal to c_0. The concentration at the membrane surface c_w, which controls the permeate velocity and is the quantity to be sought, increases with time. The permeate velocity declines with time as a result of the decrease in the process driving force, the difference between the transmembrane hydraulic pressure ΔP, and transmembrane osmotic pressure $\Delta\pi$. The latter pressure is a linear function of the salt concentration. Assume that only a small number of salt molecules can pass through the membrane, so its selectivity $R = (c_w - c_p)/c_w$, where c_p is the permeate concentration, is close to unity.

In this case, the mass transfer from the membrane surface is described by the following unsteady one-dimensional diffusion equation[13]:

$$\frac{\partial c}{\partial t} - V_0(1 - \delta c_w/c_0)\frac{\partial c}{\partial y} = D\frac{\partial^2 c}{\partial y^2} \tag{44}$$

$$t = 0 \qquad c = c_0 \qquad y = 0 \qquad D\frac{\partial c_w}{\partial y} = -V_0(1 - \delta c_w/c_0)Rc_w$$

$$y \to \infty, c \to c_0 \tag{45}$$

Here, $V_p = A(\Delta P - \Delta\pi)$ is the permeate velocity; $\Delta\pi = \pi_w - \pi_p$ is the transmembrane osmotic pressure; π_w is the osmotic pressure at the upside membrane surface; π_p is the permeate (downside membrane surface) osmotic pressure; A is the membrane permeability coefficient, $\delta = R\pi_0/\Delta P$; π_0 is the osmotic pressure at a concentration equal to c_0; V_0 is the initial permeate

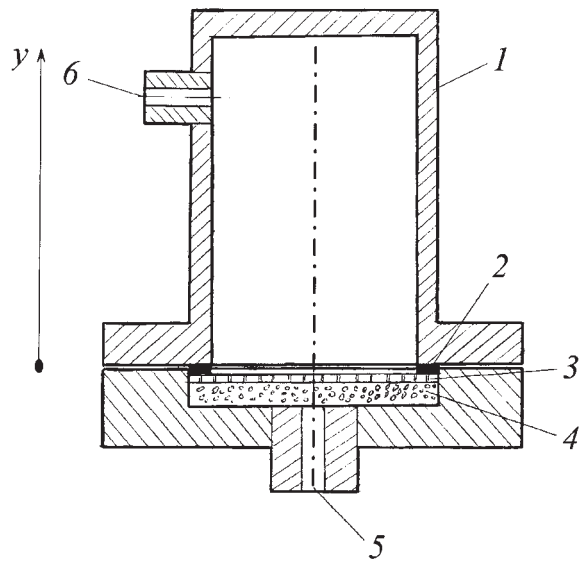

Figure 8. Unstirred reverse osmosis batch cell.

1, Housing; 2, gasket; 3, semipermeable membrane; 4, porous support; 5, permeate outlet; 6, feed inlet.

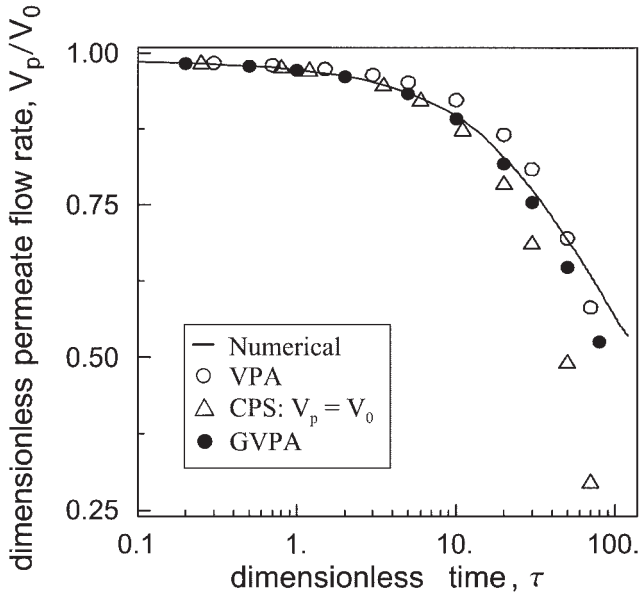

Figure 9. Decline of permeate flow rate with time.

$R = 1$, $\delta = 0.01$, $Y = 0$.

velocity; and D is the diffusion coefficient of salt molecules in water.

Equations 44 and 45 in dimensionless form are written as[13]

$$\frac{\partial C}{\partial \tau} - \frac{\partial^2 C}{\partial Y^2} = (1 - \delta C_w)\frac{\partial C}{\partial Y} \tag{46}$$

$$\tau = 0 \qquad C = 1 \qquad Y = 0 \qquad \frac{\partial C_w}{\partial Y} = -RC_w(1 - \delta C_w)$$

$$Y \to \infty, C \to 1 \tag{47}$$

Here, $\tau = V_0^2 t/D$, $Y = V_0 y/D$, $C = c/c_0$, and $C_w = c_w/c_0$.

Averaging the dimensionless permeate velocity $v = V_p/V_0$ over time yields

$$\frac{\partial C}{\partial \tau} - \frac{\partial^2 C}{\partial Y^2} = \langle v \rangle \frac{\partial C}{\partial Y} \tag{48}$$

$$\langle v \rangle = \frac{1}{\tau}\int_0^{\tau} (1 - \delta C_w) d\tau_1 \tag{49}$$

$$\tau = 0 \qquad C = 1 \qquad Y = 0 \qquad \frac{\partial C_w}{\partial Y} = -R\langle v \rangle C_w$$

$$Y \to \infty, C \to 1 \tag{50}$$

Introducing new independent variables $\lambda = Y\langle v \rangle$ and $\theta = \tau\langle v \rangle^2$ and solving the above problem with the help of Laplace transform gives the formula[13]:

$$C = 1 + \frac{R}{2(1-R)}\exp[-\lambda]\mathrm{erfc}\left(\frac{\lambda}{2\sqrt{\theta}} - \frac{\sqrt{\theta}}{2}\right) - \frac{1}{2}\mathrm{erfc}\left(\frac{\lambda}{2\sqrt{\theta}} + \frac{\sqrt{\theta}}{2}\right) - \frac{2R-1}{2(1-R)}\exp[-R\lambda - R(1-R)\theta]\mathrm{erfc}\left[\frac{\lambda}{2\sqrt{\theta}} - (2R-1)\frac{\sqrt{\theta}}{2}\right] \tag{51}$$

For $R = 1$, taking the limit in the above solution yields

$$c = 1 + \frac{1}{2}(1 + \theta - \lambda)\exp[-\lambda]\mathrm{erfc}\left(\frac{\lambda}{2\sqrt{\theta}} - \frac{\sqrt{\theta}}{2}\right) - \frac{1}{2}\mathrm{erfc}\left(\frac{\lambda}{2\sqrt{\theta}} + \frac{\sqrt{\theta}}{2}\right) + \sqrt{\frac{\theta}{\pi}}\exp\left[-\frac{(\lambda+\theta)^2}{4\theta}\right] \tag{52}$$

The dependency of $\langle v \rangle$ on time was interpolated with the help of Eq. 26.

Figures 9 and 10 illustrate the comparison between the curves of permeate velocity vs. time calculated by different methods for two values of membrane selectivity R and parameter δ. The numerical solution was taken from Bellucci and Pozzi[11] for $R = 1$ and from Bellucci et al.[32] for $R = 0.77$. Equation 51 is used for the CPS curve with $V_p = V_0$ for $R = 0.77$ and Eq. 52 for $R = 1$.

It is seen that, as in the preceding examples, the GVPA gives the least deviation from the numerical solution in the whole time interval.

Conclusions

The above study demonstrates that the GVPA method can successfully be used to solve:

(1) Nonlinear partial differential equations, including those

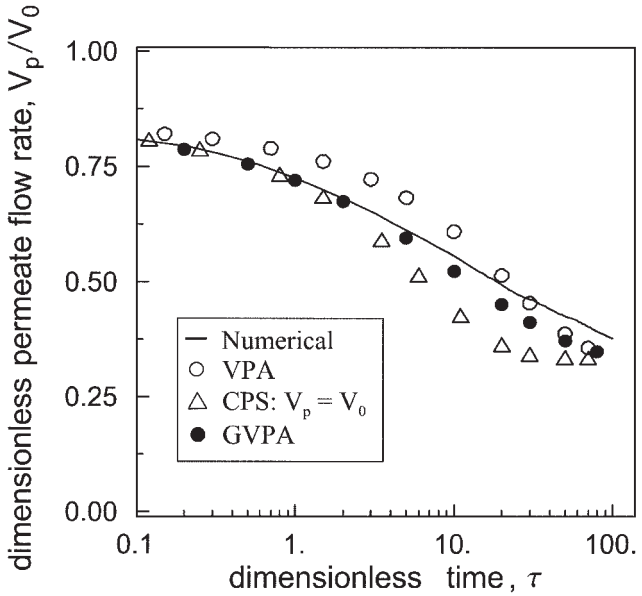

Figure 10. Decline of permeate flow rate with time.

$R = 0.77$, $\delta = 0.154$, $Y = 0$.

in which the nonlinear partial differential equation also involves the unknown function taken at the boundary.

(2) Nonlinear integrodifferential equations.

(3) Problems with nonlinear boundary conditions.

(4) Nonlinear problems with multiple occurrences of the variable parameter to be averaged.

Our analysis shows that the GVPA method can be used to solve nonlinear problems in which:

(1) The variable parameter is multiplied by a linear term, as in the case of transfer coefficients.

(2) The variable parameter is a monotonic function of the function to be determined.

(3) The process is either unsteady or steady with developing profiles.

(4) The process runs in a finite volume (filter, reactor, etc.).

(5) The constant-parameter problem has an exact, or approximate, analytical or rapid numerical solution.

Specifically, the GVPA method can be used to obtain low-error approximate solutions to pressure-driven membrane technology problems and momentum, energy, or mass-transfer equations.

The GVPA algorithm is simple to program and uses analytical or quick numerical solutions to the constant-parameter case of the original problem.

The GVPA method can provide the least error when the unknown function is an algebraic function of the variable parameter to be averaged.

Notation

A = membrane coefficient, m s^{-1} Pa^{-1}
b = constant in Eq. 37, m^3/mol
B = dimensionless constant b
C = dimensionless particle concentration in suspension, or dimensionless salt concentration in solution
C_w = dimensionless salt concentration at membrane surface
c = particle concentration in suspension, kg/m^3; or salt concentration in solution, mol/m^3
c_* = salt concentration at phase boundary, mol/m^3
c_0 = suspended particle concentration in feed slurry, kg/m^3; or salt concentration in feed solution, mol/m^3
c_f = suspended particle concentration in filtrate, kg/m^3
c_p = salt concentration in permeate, mol/m^3
c_w = salt concentration at membrane surface, mol/m^3
D = diffusion coefficient, m^2/s
$\langle D \rangle$ = averaged dimensionless diffusion coefficient
D_0 = diffusion coefficient in infinitely diluted solution, m^2/s
d = equivalent depth of modular (rectangular) hollow-fiber filter, m
H = thickness of diffusion boundary layer, m
I_m = modified Bessel function of order m
N_α = dimensionless number given by the ratio of desorption and adsorption rate constants
N_β = dimensionless number accounting for the adsorption ability of membrane surface with respect to suspended particles
N_β^* = averaged value of N_β ($=N_\beta/\langle v \rangle$)
N_χ = dimensionless number accounting for cake and membrane resistance ($=\chi_1 c_0/s$)
ΔP = transmembrane pressure, Pa
R = rejection coefficient (selectivity) for reverse osmosis membrane
R_m = clean membrane resistance, m^{-1}
r = radial coordinate, m
r_0 = external radius of hollow-fiber bundle in radial filter, m
r_c = specific cake resistance, m/kg
r_{in} = internal radius of hollow-fiber bundle in radial filter, m
s = specific membrane surface area in filter, m^{-1}
t = time, s
V = permeate velocity averaged over filter depth, m/s
V_0 = initial permeate velocity, m/s
V_p = permeate velocity, m/s
v = dimensionless permeate velocity
$\langle v \rangle$ = averaged dimensionless permeate velocity
w = filtration velocity, m/s
w_0 = feed velocity, m/s
X = dimensionless corrected coordinate
Y = dimensionless vertical coordinate
y = vertical coordinate, m
Z = dimensionless effective filter depth coordinate
z = effective filter depth coordinate, m

Greek letters

α = desorption (reentrainment) coefficient, s^{-1}
β = adsorption (deposition) coefficient, m/s
Γ = specific cake deposit, kg/m^2
γ = dimensionless specific cake deposit
μ = fluid viscosity, Pa·s
ξ = ratio of initial permeate flow rate to feed flow rate
ξ_{av} = average ratio of permeate flow rate to feed flow rate
$\Delta\pi$ = osmotic pressure difference across membrane ($=\pi_w - \pi_p$), Pa
π_0 = osmotic pressure corresponding to $c = c_0$, Pa
π_p = permeate osmotic pressure, Pa
π_w = osmotic pressure at membrane surface, Pa
τ = dimensionless time
χ_1 = ratio of specific cake resistance to clean membrane resistance ($=r_c/R_m$), m^2/kg

Literature Cited

1. Reynolds J, Jeris JS, Theodore L. *Handbook of Chemical and Environmental Engineering Calculations.* New York, NY: Wiley; 2002.
2. Finlayson BA. *Introduction to Chemical Engineering Computing.* New York, NY: Wiley; 2006.
3. Kutepov AM, ed. *Protsessy i Apparaty Khimicheskoi Teckhnologii* (Unit Operations of Chemical Engineering). Moscow, Russia: Logos; 2000;1–2 (in Russian).
4. Polyanin AD, Dilman VV. *Methods of Modeling Equations and Analogies in Chemical Engineering*. Boca Raton, FL: CRC Press; 1994.
5. Polyanin AD, Zaitsev VF. *Handbook of Nonlinear Partial Differential Equations.* Boca Raton, FL: CRC Press; 2004.
6. Hoffman JD. *Numerical Methods for Engineers and Scientists.* 2nd Edition. New York, NY: Marcel Dekker; 2001.
7. Samarskii AA, Vabishchevich PN. *Computational Heat Transfer.* New York, NY: Wiley; 1996;1–2.
8. Zwillinger D. *Handbook of Differential Equations.* 3rd Edition. Boston, MA: Academic Press; 1997.
9. De S, Bhattacharjee S, Sharma A, Bhattacharya PK. Generalized integral and similarity solutions of the concentration profiles for osmotic pressure controlled ultrafiltration. *J Membr Sci.* 1997;130:99-121.
10. Polyakov SV, Volgin VD, Maksimov ED, Laziev SP. Methods of calculating the concentration field in unstirred reverse osmosis cells. *Khim Tekhnol Vody* (*J Water Chem Technol*). 1982;4:203-208 (in Russian).
11. Bellucci F, Pozzi A. Numerical and analytical solutions for concentration polarization in hyperfiltration without axial flow. *Int J Heat Mass Transfer.* 1975;18:945-951.
12. Nayfeh AH. *Introduction to Perturbation Techniques.* New York, NY: Wiley; 1993.
13. Liu MK, Williams FA. Concentration polarization in an unstirred batch cell: Measurements and comparison with theory. *Int J Heat Mass Transfer.* 1970;13:1441-1457.
14. Polyakov SV, Volgin VD, Maksimov ED, Sinyak YuE. Calculation of concentration polarization in reverse osmosis plants with flat channel membrane elements. *Khim Tekhnol Vody* (*J Water Chem Technol*). 1982;4:299-304 (in Russian).
15. Schlichting H, Gersten K. *Boundary Layer Theory.* 8th Edition. New York, NY: Springer-Verlag; 2004.
16. Berman AS. Laminar flow in channels with porous walls. *J Appl Phys.* 1953;24:1232-1235.
17. Sherwood TK, Brian PLT, Fisher RE, Dresner L. Salt concentration at phase boundaries in desalination by reverse osmosis. *Ind Eng Chem Fundam.* 1965;4:113-118.

18. Ruckenstein E, Prieve DC. Rate of deposition of Brownian particles under the action of London and double-layer forces. *J Chem Soc Faraday Trans II.* 1973;69:1522-1536.
19. Spielman AL, Friedlander SK. Role of the electrical double layer in particle deposition by convective diffusion. *J Colloid Interface Sci.* 1974;46:22-31.
20. Prieve DC, Lin MMJ. Adsorption of Brownian hydrosols onto a rotating disc aided by a uniform applied force. *J Colloid Interface Sci.* 1980;76:32-47.
21. Dresner L. *Boundary Layer Build-Up in the Demineralization of Salt Water by Reverse Osmosis.* Report 3621, May. Oak Ridge, TN: Oak Ridge National Laboratory; 1964.
22. Polyanin AD, Kutepov AM, Vyazmin AV, Kazenin DA. *Hydrodynamics, Mass and Heat Transfer in Chemical Engineering.* London, UK: Taylor & Francis; 2002.
23. Polyanin AD, Manzhirov AV. *Handbook of Integral Equations.* Boca Raton, FL: CRC Press; 1998.
24. Vyaz'min AV, Denisov IA, Polyanin AD. Method of asymptotic interpolation in problems of chemical hydrodynamics and mass transfer. *Theor Found Chem Eng.* 2001;35:1-8.
25. Polyakov YuS. Membrane separation in dead-end hollow fiber filters at constant transmembrane pressure. *Theor Found Chem Eng.* 2005; 39:471-477.
26. Polyakov YuS. Dead-end outside-in hollow fiber membrane filter: Mathematical model. *J Membr Sci.* 2006;279:615-624.
27. Polyakov YuS. Particle deposition in outside-in hollow fiber filters and its effect on their performance. *J Membr Sci.* 2006;278:190-198.
28. Polyakov YuS, Kazenin DA. Membrane filtration with reversible adsorption: Outside-in hollow fiber membranes as collectors of colloidal particles. *Theor Found Chem Eng.* 2005;39:118-128.
29. Polyakov YuS, Kazenin DA. Membrane filtration with reversible adsorption: The effect of transmembrane pressure, feed flow rate, and geometry of hollow fiber filters on their performance. *Theor Found Chem Eng.* 2005;39:402-406.
30. Polyakov YuS, Kazenin DA. Nonlinear mass transfer with reversible adsorption on semipermeable membranes in membrane adsorbers. *Proceedings of the 18th International Science Conference: Mathematical Methods in Engineering.* Kazan, Russia: Kazan State Technical Univ.; 2005;1:156-160 (in Russian).
31. Reid RC, Prausnitz JM, Polling BE. *The Properties of Gases and Liquids.* New York, NY: McGraw-Hill; 1987.
32. Bellucci F, Drioli E, Pozzi A. Flow regimes in an unstirred discontinuous hyperfiltration process: Comparison between theoretical and experimental results. *Desalination.* 1975;16:287-301.

Manuscript received Jan. 21, 2006, and revision received Aug. 3, 2006.